Structural Basis for Recruitment of Rab6-Interacting Protein 1 to Golgi via a RUN Domain

Rosario Recacha,[1] Annick Boulet,[2] Florence Jollivet,[2] Solange Monier,[2,3] Anne Houdusse,[2] Bruno Goud,[2] and Amir R. Khan[1,*]

[1]School of Biochemistry and Immunology, Trinity College, Dublin 2, Ireland
[2]UMR 144 CNRS/Institut Curie, Institut Curie, 75248 Paris Cedex 5, France
[3]Present address: UMR 6061 CNRS/Université de Rennes, Rennes, France
*Correspondence: amirrafk@tcd.ie

SUMMARY

Small GTPase Rab6 regulates vesicle trafficking at the level of Golgi via recruitment of numerous and unrelated effectors. The crystal structure of Rab6a(GTP) in complex with a 378-residue internal fragment of the effector Rab6IP1 was solved at 3.2 Å resolution. This Rab6IP1 region encompasses an all α-helical RUN domain followed in tandem by a PLAT domain that adopts a β sandwich fold. The structure reveals that the first and last α helices of the RUN domain mediate binding to switch I, switch II, and the interswitch region of Rab6. It represents the largest Rab-effector complex determined to date. Comparisons with the recent structure of Rab6 in complex with an unrelated effector, human golgin GCC185, reveals significant conformational changes in the conserved hydrophobic triad of Rab6. Flexibility in the switch and interswitch regions of Rab6 mediates recognition of compositionally distinct α-helical coiled coils, thereby contributing to Rab6 promiscuity in effector recruitment.

INTRODUCTION

The architecture of eukaryotic cells consists of a complex assortment of subcellular compartments and the underlying cytoskeletal network. The nucleus, endoplasmic reticulum (ER), Golgi apparatus, mitochondria, and a variety of vesicular bodies perform coordinated exchange of cargo throughout the life cycle of cells. The p21 Ras superfamily of small GTPases are spatial/temporal switches that choreograph diverse processes such as organelle dynamics, cell proliferation, chemotaxis, synaptic transmission, and cytokinesis (Goldfinger, 2008).

The complexity of eukaryotic intracellular trafficking is reflected in the evolutionary diversity of *rab* genes, which are considered the premier organizers of membranes and vesicle trafficking pathways (Zerial and McBride, 2001). Rab GTPases comprise the largest member of the Ras superfamily with nearly 70 proteins, several of which are conserved from yeast to humans (Stenmark and Olkkonen, 2001). Following biosynthesis,

Rabs are guided to their cognate membranes via interactions with Rab escort protein (REP), which is an essential accessory protein for subsequent prenylation of C-terminal Cys residues by geranylgeranyl transferase (GGTase) (Andres et al., 1993; Farnsworth et al., 1991; Goody et al., 2005). Rabs oscillate between inactive (GDP-bound) cytosolic, and active (GTP-bound) membrane-associated states, and this cycle is regulated by several accessory proteins. GDP dissociation inhibitors (GDIs) trap Rabs in the inactive state and participate in the membrane association/dissociation process (Wu et al., 1996), GDP/GTP exchange factors (GEFs) activate Rabs by promoting nucleotide exchange (Geyer and Wittinghofer, 1997), and GTPase activating proteins (GAPs) accelerate hydrolysis of the γ-phosphate of bound GTP (Geyer and Wittinghofer, 1997).

Active Rabs interact with the Rab-binding domain (RBD) of their cognate effectors to recruit them to specific subcellular compartments. Each Rab interacts with a unique subset of effector proteins, often unrelated in sequence and structure. Effectors are typically multidomain proteins that, in addition to the RBD, also contain additional domains that mediate biological effects upon Rab recruitment. Thus, a snapshot of the cell would reveal the dynamic association of innumerable Rab-effector complexes regulating the exchange of cargo between subcellular compartments. The Structural Genomics Consortium along with independent labs has collectively determined the structures of most Rabs in the human genome. All known Rabs except inactive Rab27 (Chavas et al., 2007) share an identical α/β Ras superfamily fold. However, only seven sets of Rab-effector crystal structures are known: (i) Rab3-Rabphilin-3 (Ostermeier and Brunger, 1999), which delivers secretory granules in several cell types, although the biologically relevant complex is probably Rab27-Rabphilin-3 (Fukuda, 2006); (ii) Rab5-rabaptin5 (Zhu et al., 2004), involved in early endosome fusion; (iii) Rab7-RILP (Rab7-interacting lysosomal protein) (Wu et al., 2005), which regulates fusion between lysosomes and endosomes; (iv) Rab4/Rab22 each with rabenosyn5 (Eathiraj et al., 2005), involved in coordinating endosomal traffic through simultaneous complex formation with Rab5; (v) Rab11-FIP2 (Rab11-family interacting protein 2) from our group (Jagoe et al., 2006), and Rab11-FIP3 from two other labs (Eathiraj et al., 2006; Shiba et al., 2006), which regulate endocytic recycling pathways; and (vi) Rab6 in complex with the RBD of GCC185, a golgin involved in endosome to Golgi transport and maintenance of Golgi
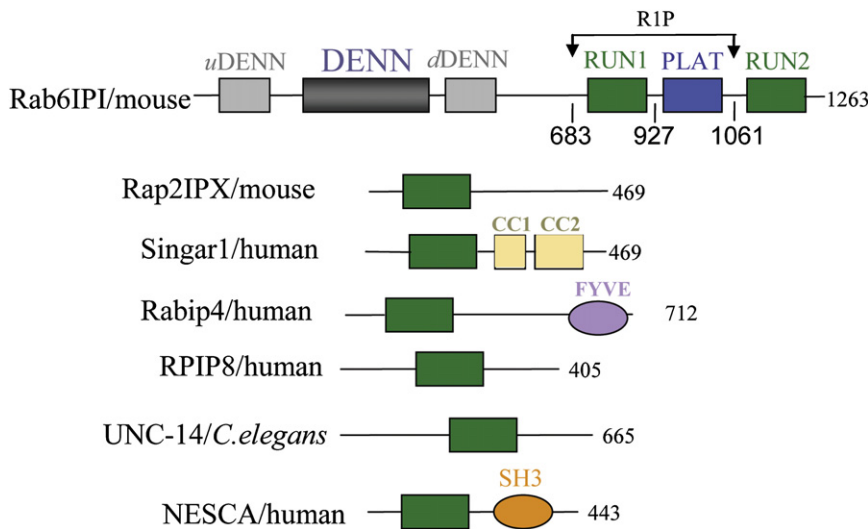
Figure 1. Domain Organization of RUN-Domain-Containing Signaling Proteins

DENN indicates *d*ifferentially *e*xpressed in *n*eoplastic versus *n*ormal cells; *u*DENN, *upstream* DENN ; *d*DENN , *downstream* DENN; CC1 and CC2, coiled coil regions; FYVE, *F*ab1, *Y*OTB, *V*ac1, and *E*EA1 zinc finger domain; SH3, *S*rc *homology 3* domain.

Rab6IP1, originally called *orf37* (open reading frame 37), was identified as a Rab6(GTP)-specific binding protein using a yeast two-hybrid screen of a mouse brain cDNA library (Janoueix-Lerosey et al., 1995). Two isoforms, termed Rab6IP1A and Rab6IP1B and differing by a stretch of 24 amino-acids at their N termini, are ubiquitously expressed in mammals (Miserey-Lenkei et al., 2007). The relative expression of each isoform depends on tissues and cell types (Miserey-Lenkei et al., 2007). Endogenous Rab6IP1 is a cytosolic protein recruited by active Rab6 (Rab6:GTP) onto Golgi membranes (Miserey-Lenkei et al., 2007). Rab6IP1 also binds to Rab11 in a GTP-dependent manner, suggesting that Rab6IP1 links the functions of Rab6 and Rab11 in transport events between Golgi and endosomes (Miserey-Lenkei et al., 2007).

The primary sequence of Rab6IP1 reveals a modular organization typical of many Rab effectors (Figure 1). Previous deletion studies narrowed the Rab6-binding segment to 683–1061, which spans the first RUN domain (RUN1) of Rab6IP1, followed by a PLAT domain (Miserey-Lenkei et al., 2007). RUN domains are widespread in cytosolic proteins and are presumed to have diverse roles in cellular signaling (Callebaut et al., 2001; Mori et al., 2007). The RUN acronym was coined after three members of the family: the RPIP8 protein, an effector of Rap2 (Bourne et al., 1991); UNC-14, a protein that plays a role in axonal elongation and guidance in *C. elegans* (Ogura et al., 1997); and NESCA (*ne*w molecule containing *S*H3 domain at the *ca*rboxy terminus), an SH3 domain-containing protein cloned from human placental cells. A common feature of some of these proteins is their link to small GTPase functions (Rab6IP1, Rap2-IPX, Rabip4). Recently, the isolated crystal structure of the RUN domain of Rap2IPX revealed an 8-helix bundle with a novel topology, but the complex with its signaling partner remains to be determined (Kukimoto-Niino et al., 2006). The PLAT domain, also referred to as LH2 (lipoxygenase homology domain 2) (Bateman and Sandford, 1999), was named after three members in which this motif was discovered: polycystin-1, the product of polycystic kidney disease 1 (*PKD1*) associated with renal cysts and kidney disease (Sandford et al., 1997); lipoxygenases, multi-subunit enzymes involved in the biosynthetic pathway of hormones from lipid substrates (Gillmor et al., 1997); and alpha-toxin, a pore-forming molecule expressed by pathogenic bacteria. The function of this β sandwich domain remains ill-defined, although it is generally observed in proteins that interact with phospholipid bilayers and there is experimental support for roles in protein-protein and protein-lipid interactions (Aleem

structure (Burguete et al., 2008; Derby et al., 2007). Finally, the structures of Rab27B and Rab27A in complex with the RBDs of two different effectors (Rab27B-slac2-a/melanophilin, 140-residue RBD; Rab27A-Slp2a, 50-residue RBD) have also recently been deposited in the Protein Data Bank (Chavas et al., 2008). Without exception, all known Rab-effector complexes are characterized by one or two α helices from the RBD of the effector in intimate contact with the GTP-sensitive switch I/II regions from the cognate Rab. Apart from Rabphilin-3 and melanophilin (120–140 residues), the short RBDs from Rab-effector structures (40–60 residues) might appropriately be termed α-helical "motifs" rather than domains. In addition, a strictly conserved aromatic triad from Rabs (Phe in switch I, Trp in the interswitch, and Tyr/Phe in switch II) contributes to the binding interface with effectors. The side-chain conformations of the triad are variable, and this conformational heterogeneity is believed to contribute to Rab-effector specificity (Eathiraj et al., 2005; Merithew et al., 2001).

Rab6 regulates transport pathways at the level of Golgi. Three members of the Rab6 family have been identified to date: Rab6a, Rab6a′ (which is a splicing variant of a duplicated exon, differing from Rab6A by 3 residues), and Rab6b, which is preferentially expressed in a subset of neuronal cells (Darchen and Goud, 2000; Opdam et al., 2000). Using the transport of Shiga toxin B-subunit as a model system, it has been shown that Rab6 regulates endosome-to-Golgi and Golgi-to-ER retrograde transport pathways (Del Nery et al., 2006; Mallard et al., 2002; White et al., 1999). A role for Rab6 in the organization of exocytic vesicles that are delivered from the Golgi apparatus to the cell membrane has also been recently documented (Grigoriev et al., 2007). In addition, a small interfering RNA (siRNA) screen has linked Rab6 regulation of Golgi retrograde pathways to human immunodeficiency virus entry and productive infection (Brass et al., 2008). Several unrelated Rab6 effectors have been identified using various genetic and biochemical approaches, including subunits of the dynein/dynactin complex, Rabkinesin-6/MKIP2, GAPCenA, Rab6IP2/ELKS, TMF/ARA160, and mint3 (Cuif et al., 1999; Echard et al., 1998; Fridmann-Sirkis et al., 2004; Miserey-Lenkei et al., 2006; Short et al., 2002; Teber et al., 2005).

et al., 2008; Bateman and Sandford, 1999; Hu and Barr, 2005; Ponting et al., 1999).

In order to understand the structural basis for Rab-effector specificity and function, we have determined the crystal structure of the 378-residue RUN1-PLAT fragment of Rab6IP1 in complex with Rab6 by single-wavelength anomalous diffraction (SAD) methods. The structure reveals that Rab6 binding is mediated by noncontiguous α1 and α8 of the RUN1 domain. Comparison with the structure of Rab6 in complex with the human golgin protein GCC185 shows similarities in the nature of the Rab-effector interface and topology of the two effector α helices. However, the strictly conserved aromatic triad of Rab6 reveals conformational flexibility in adapting to the hydrophobic interface presented by two unrelated effectors, which has not been described previously in Rab-effector complexes.

RESULTS

Identification of the Rab6-Binding Segment of Rab6IP1

Yeast two-hybrid analyses and GST-pull down experiments had previously established that the minimal Rab6 binding segment of mouse Rab6IP1 comprises residues 683–1061 (Figure 1), which encompass a tandem RUN1-PLAT domain organization (Miserey-Lenkei et al., 2007). This segment of RUN1-PLAT, which will henceforth be referred to as "R1P", is indistinguishable between the Rab6IP1A and Rab6IP1B isoforms. We subcloned the R1P fragment into various *Escherichia coli* vectors, but all attempts at soluble expression failed. Coexpression of R1P with human Rab6a (residues 8–195, Q72L mutant) resulted in a soluble complex that crystallized in a hexagonal space group P6₁22, with one Rab6-R1P complex in the asymmetric unit. Static light scattering indicated a 1:1 complex of Rab6 and R1P in solution (see Figure S1 available online). Once the crystal structure was solved, it was evident that Rab6-R1P interactions are mediated solely by its RUN1 domain in the final refined model. We designed various constructs to independently express RUN1, either alone or together with Rab6. However, all expression strategies to generate RUN1 alone or in complex with Rab6 failed to produce soluble RUN1 protein in *E. coli*. Furthermore, yeast two-hybrid analyses of RUN1 and Rab6 failed to show an interaction (Table S2). Possible explanations for these observations will be discussed below.

Structure of R1P

The RUN1 domain is a 9-helix bundle that is dominated along one side by the 33-residue N-terminal α helix (Figure 2). Most of the α helices pack together with antiparallel or perpendicular topology, organized roughly into a Greek key resembling the death domain family. One notable exception is the pair of helices α1/α8 that are parallel and which form the Rab6 binding interface. In the complex Rab6-R1P, interactions with Rab6 are mediated exclusively via RUN1. The structure of RUN1 is similar to the recently determined crystal structure of the isolated RUN domain from Rap2IPX (Kukimoto-Niino et al., 2006), with an root-mean-square deviation (rmsd) of 1.83 Å over 162 Cα atoms (23% sequence identities). The structure of Rap2IPX was determined after optimization of soluble protein expression using NMR heteronuclear single-quantum coherence experiments of various fragments of the RUN domain. These NMR studies suggested
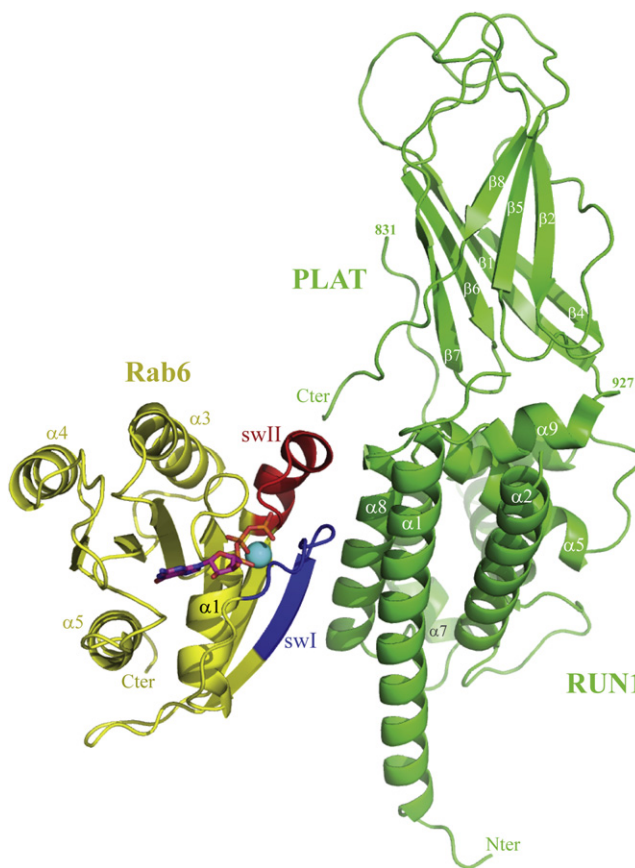

Figure 2. Ribbon Model of the Rab6-Rab6IP1 Complex
Switch I is colored blue, and switch II is red. Interactions with Rab6 are restricted to α1 and α8 of the RUN1 domain. The intervening helix α9 (residues 919–926) mediates intimate contacts with the all-helical RUN1 domain and loops from the PLAT β sandwich.

that the globular portion of the RUN domain extends further toward the N terminus than predicted by the initial bioinformatics studies of the RUN domain family (Callebaut et al., 2001). Subsequently, the crystal structure of Rap2IPX revealed that this region adopts the N-terminal helix that is presumably essential for correct folding of the RUN domain, and due to poor sequence conservation, it was overlooked in multiple sequence alignments. Interestingly, the equivalent N-terminal helix of R1P is one of the two helices that binds to Rab6.

The main differences in the two RUN domains are localized to the α3-α4 loop and the C terminus (Figure 3). The long axis of α3 in R1P is rotated about 36° relative to α3 of Rap2IPX, despite a conserved Trp hydrophobic anchor (Trp794 in RUN1) at the base of the helices. A tight turn linking α3-α4 in Rap2IPX, aided by Pro159 in the loop, may explain the closer packing of the two helices in Rap2IPX. In contrast, there is a 32-residue insertion in the α3-α4 loop of R1P, the majority of which is disordered (residues 809-830 of RUN1). Following α8, the two RUN domains share a common C-terminal helix (α9), but their backbones follow very different paths relative to each other. The α9 of R1P is sandwiched between the globular RUN1 domain and the subsequent PLAT domain (Figure 3), whereas the C-terminal helix of Rap2IPX extends away from the globular portion of the
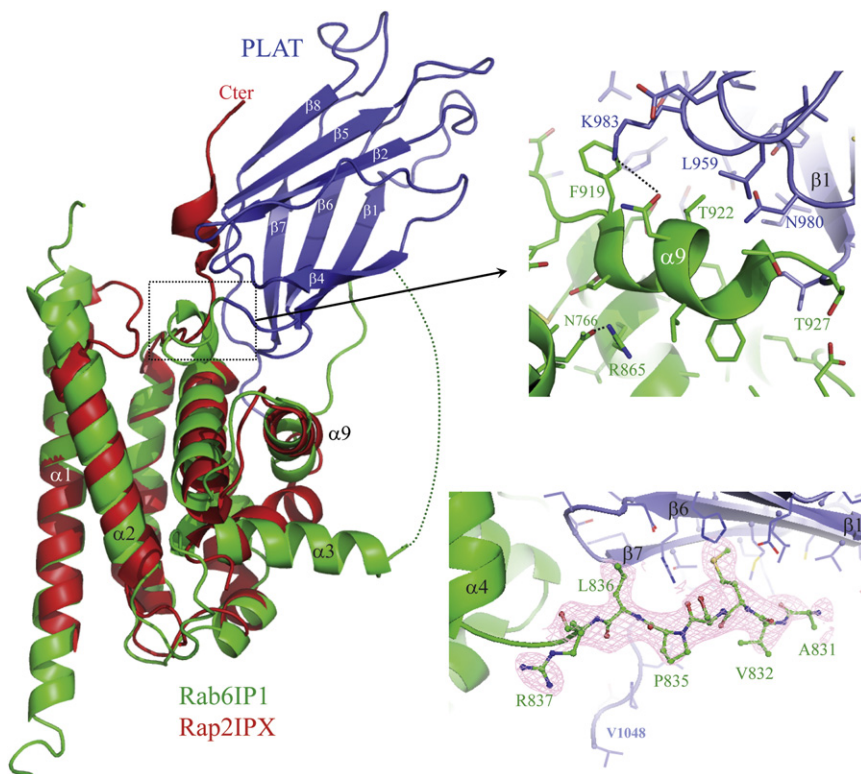
Figure 3. Superposition of the RUN Domains of Rab6IP1 and Rap2IPX
The PLAT domain of Rab6IP1 is colored blue (residues Ile928–Val1048) to distinguish it from the RUN1 domain (Asn713–Thr927) of Rab6IP1. Extensive polar and nonpolar interactions are evident between the loops connecting the β sandwich of the PLAT domain with the short intervening helix (α9) that packs against the globular RUN1 domain. This intervening α helix, which buffers the interactions with PLAT, is not conserved in the RUN domain of Rap2IPX (red).
(Right, bottom) Part of the loop connecting α3 and α4 of RUN1 (residues 831–837) is modeled on the surface of the β sheet of the PLAT domain, thereby reinforcing the interactions between the two domains. The electron density (2F$_o$-F$_c$) is contoured at 1σ.

such that two noncontiguous α helices α1/α8 of Rab6IP1 form the Rab-binding interface, unlike Rab11-FIP2, Rab6-GCC185, and Rab5-rabaptin5 in which parallel α helices are formed through dimerization of the effectors. Rab7-RILP, like the present structure, is a 1:1 complex, but the RBD is a contiguous segment of polypeptide in which the two α helices have antiparallel topology, and only one helix interacts with Rab7.

The switch and interswitch residues of Rab6 that recognize Rab6IP1 are highly conserved among human Rabs. However, one of the key determinants of specificity is Lys13 of Rab6, which resides on β1 and forms a salt bridge with Asp901. Lys13 is a hydrophobic residue in other human Rabs (Figure 5), but apart from this, all other residues that interact with R1P are either identical or conservative changes in other Rab proteins. The apparent dilemma in Rab-effector specificity is resolved by variability in the three-dimensional spatial position and conformation
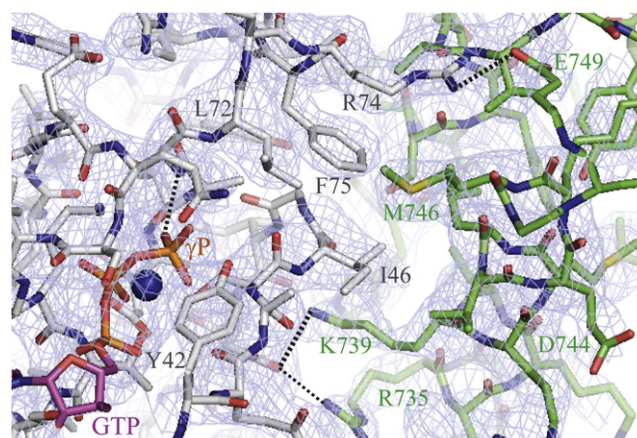
molecule. Intriguingly, in R1P there are extensive hydrophobic interactions between the loops from PLAT and α9, α4, and α5 of the RUN1 domain. Furthermore, part of the loop preceding α4 (residues 831–836) has been modeled on the surface of the PLAT domain (Figure 3), guided by a continuous stretch of electron density and the presence of a SeMet (Met833) as an anchor upon inspection of electron density maps. These interactions lead to a tight association of RUN1 and PLAT domains, so that the tandem RUN1-PLAT segment of Rab6IP1 can be considered a rigid two-domain module. These structural properties might explain the apparent instability of smaller R1P fragments, in particular the inability to express a soluble complex of the RUN1 domain with Rab6.

Rab6 Interface with RUN1 and Rab-Effector Specificity

A hydrophobic interface involving residues from switch I/II and the interswitch of Rab6 (Ile46, Ile48, Phe50, Trp68, Phe75, Leu78, and Tyr82) packs against the parallel α1/α8 helices of RUN1 (Figures 4 and 5). Both RUN1 α helices supply charge complementarity with Rab6, forming ion pairs Lys13-Asp901, Arg74-Glu749, whereas Asp49 is in the neighborhood of both Arg735 and Lys739. The key determinant in GTP specificity is the "IGIDF" motif of switch I, whose conformation is influenced by the presence of γ-phosphate, and which resides in the α1/α8 interface, contributing both hydrophobic interactions and a salt bridge. The overall buried surface area in the complex is 1506 Å^2. The nature of the binding interface can be described as a central hydrophobic core, bordered by charge complementarity (Figure 6). In this respect, the complex resembles very much the complexes Rab11-FIP2 and Rab11-FIP3 in the overall mode of recognition. However, the Rab6-R1P complex is organized

Figure 4. Electron Density (2F$_o$-F$_c$, 1.0σ) at the Rab6-R1P Interface
Rab6 is gray (left), α1/α8 helices of R1P are green, and the blue Mg^{2+} ion, adjacent to GTP (magenta), is represented as a sphere.
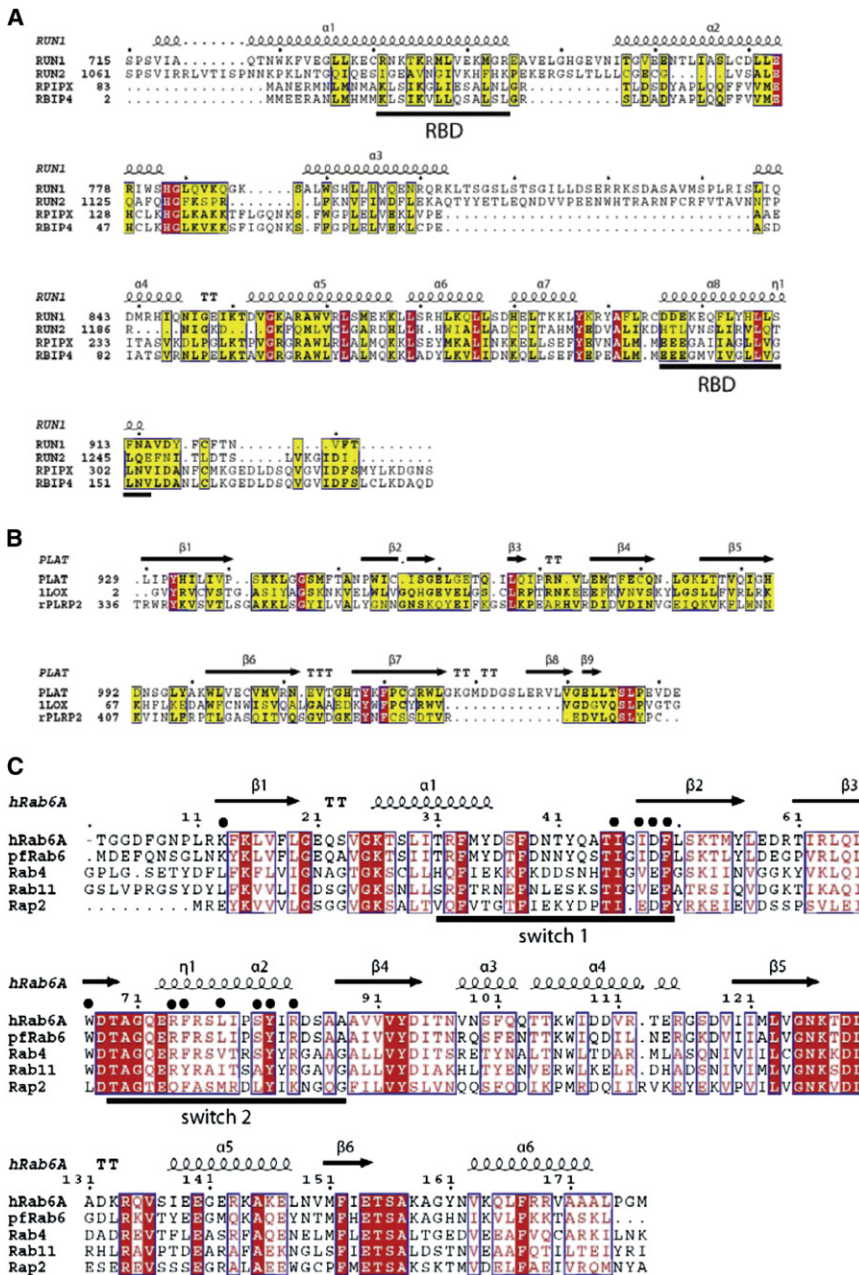
Cell PRESS

Figure 5. Sequence Alignments of RUN1, PLAT, and Human Rabs

The secondary structures corresponding to the Rab6-R1P structure are marked above the sequences. The two α helices that interact with Rab6 (A) are labeled RBD (Rab-binding domain) for convenience. The arrows (B) mark the β strands of the PLAT domain. The residues from Rab6 (C) that interact with R1P are indicated with black dots (•) above the single-letter codes. The smaller black dots indicate every tenth residue in the sequences (1, 11, 21, etc.). The variable tails of Rabs have been excluded from the alignment.

(Miserey-Lenkei et al., 2007) (Figure 7, upper panel). Depletion of Rab6 by siRNA results in a cytosolic localization of GFP-Rab6IP1, suggesting that Rab6 recruits Rab6IP1 on Golgi membranes. In support of the structural model of Rab6-R1P, we have introduced a single site mutation on α8 (K739E) in full-length Rab6IP1, as well as a double mutation on α1 (Y908S+L911A). Tyr908 interacts with the invariant Trp67 of the Rab6 aromatic triad, and along with Leu911, forms part of the hydrophobic interface. Lys739 of Rab6IP1 forms a salt bridge with Asp49 from switch I. As shown in Figure 7 (middle and lower panels), the two mutants failed to be efficiently targeted to Golgi membranes and remained cytosolic, indicating that Lys739, Tyr908, and Leu911 are crucial for Rab6-R1P interaction in vivo. In addition, yeast two-hybrid analyses revealed that the mutant Rab6(I46E) failed to interact with Rab6IP1 (Table S2). Ile46 from switch I is located at the interface of helices α1/α8 of Rab6IP1 in the complex, thus forming key hydrophobic contacts that would be destabilized in the mutant protein. Altogether, the above experiments indicate that the interactions between Rab6 and the RUN1 domain of Rab6IP1 are required for Rab6-dependent recruitment of Rab6IP1 on Golgi membranes.

of conserved switch and interswitch residues, which cannot be deduced from phylogenetic relationships in their DNA and protein sequences (Collins, 2005). Conformational variability in the switch and interswitch regions of active Rabs is now well documented in numerous crystal structures, despite their high sequence conservation (Eathiraj et al., 2005, 2006; Jagoe et al., 2006; Shiba et al., 2006). Thus, the overall scaffold supporting the switch regions influences the "exquisitely" specific interactions with effectors.

Mutations in the RUN1 Domain Impair Recruitment of Rab6IP1 to Golgi Membranes

When expressed in HeLa cells, green fluorescent protein (GFP)-tagged wild-type Rab6IP1 is targeted to Golgi membranes

DISCUSSION

Comparisons of Rab6-Rab6IP1 with Rab6-GCC185

The structure of human Rab6a (Q72L, GTP-bound) was recently determined in complex with the golgin GCC185. This complex is organized as a heterotetrameric Rab6-(GCC185)$_2$-Rab6 complex with the 37 residues of GCC185 forming the central parallel coiled coil (Figure 8). Therefore, the two complexes allow an unprecedented opportunity to compare the structural basis for recruitment of two unrelated effectors. There are similarities in the two complexes: both involve two parallel α helices in
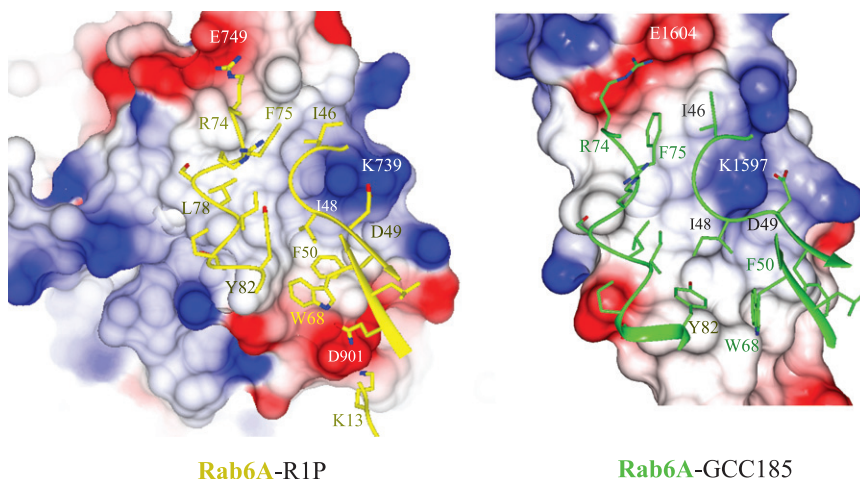
Rab6A-R1P   **Rab6A**-GCC185

Figure 6. Electrostatic and Hydrophobic Complementarity in Rab6-Effector Complexes

Rab6A in the Rab6-R1P complex is on the left (yellow ribbons/sticks), whereas Rab6A in the Rab6-GCC185 complex is on the right side (green ribbons/sticks). The Rabs are docked onto the electrostatic surface of the effectors (red, negative charge; blue, positive charge).

roughly the same arrangement against the switch and inter-switch regions of Rab6. Arg74 makes electrostatic contacts in both complexes, although to different α helices upon structural alignment, and there is a hydrophobic interface formed by both α helices from the effector (Figure 6). Tyr908 of Rab6IP1 is roughly the equivalent of Ile1588 in GCC185, mediating hydrophobic contacts with switch II. The buried surface is 1250 Å^2 for each side of the Rab6-GCC185 complex, compared with 1506 Å^2 for the single Rab6-R1P interface.

Despite a general resemblance in the mode of binding, the Rab6-complementary patches of RUN1 and GCC185 bear no compositional or structural resemblance to each other. In order to recruit two unrelated effectors, there is a conformational rearrangement in the hydrophobic triad of Rab6 (Phe50, Trp67, Tyr82; Figure 9 and Table S1). These dramatic changes take place in the context of modest conformational changes in the other interacting residues from Rab6. The rmsd for the backbone of 158 aligned Rab6 residues by secondary structure matching

was 1.07 Å. Phe50 in the Rab6-R1P complex is packed between Gln905 and Tyr908 from one helix (α8), whereas Phe50 in the Rab6-GCC185 complex packs against the other helix of GCC185 (Met1590). Trp67 forms a key hydrophobic interface with the equivalent α helix in both complexes, forming interactions with Tyr908 of R1P (α8) and Thr1585/Ile1588 in GCC185. Comparisons with uncomplexed Rab6(GTP) reveal that the triad conformation resembles that found in the Rab6-GCC185 complex. Binding of Rab6(GTP) to R1P would entail large rotations about the χ1 dihedral angle for Phe50 and Trp67 (Table S1). Although there are also significant conformational changes in Tyr82 (switch II), analyses of this region are complicated by the well-documented intrinsic flexibility of switch II (Bergbrede et al., 2005). Indeed, there is a rigid-body movement of the switch II helix in the aligned Rab6 molecules from the two complexes, placing the C_α atoms of Tyr82 about 1.8 Å apart from each other.

Previously, conformational heterogeneity in the triad has been observed between different Rabs in their active state, presumably as a consequence of the compositional and structural diversity in the underlying hydrophobic core (Merithew et al., 2001). Here we find conformational flexibility within the hydrophobic
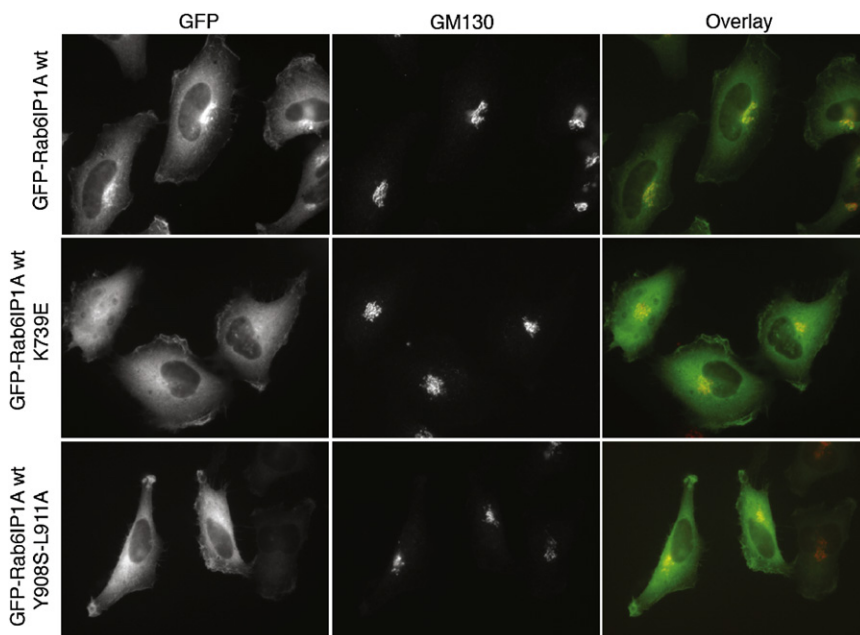

Figure 7. Mutagenesis of Rab6IP1 and Cellular Localization

Hela cells were transfected with GFP-Rab6IP1A wild-type (WT), GFP-Rab6IP1A(K739E), or GFP-Rab6Ip1A(Y908S+L911A) for 48 hr. Cells were fixed and labeled with an antibody directed against the Golgi marker.
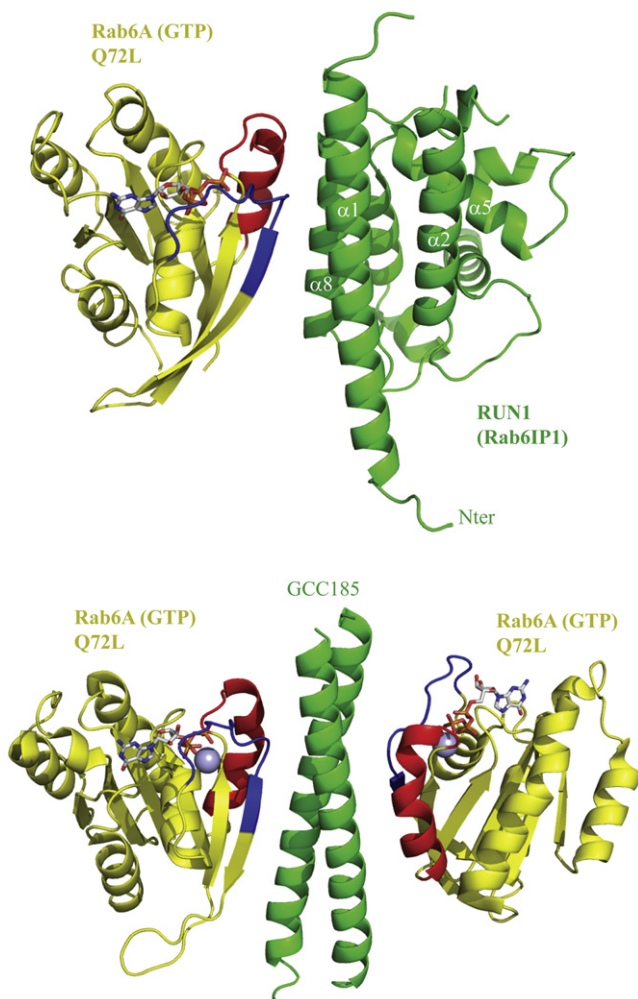
Figure 8. Comparisons of the Structures of Rab6-R1P and Rab6-GCC185

The R1P model has been stripped of the PLAT domain for clarity. A similar orientation and color scheme is shown to emphasize the similarities and differences in the overall organization of the two complexes.

triad of Rab6, enabling recruitment of unrelated effectors to Golgi. Currently, the structural basis for the conformational rearrangements is unknown. It is unclear whether effector binding shapes the conformation of the triad, or whether the aromatic residues are inherently flexible and a particular conformation is captured by the distinctive interface of the effector. As an example, Phe48 of Rab11 is observed in two distinct conformations, depending on the presence of GTPγs or GppNHp at the nucleotide binding site (Figure 9). Detailed thermodynamic and biophysical studies may distinguish the underlying mechanisms involved in effector recruitment. In concert with the apparent intrinsic flexibility of switch II regions in many Rabs (Bergbrede et al., 2005; Jagoe et al., 2006), these structural properties might explain the promiscuity of Rabs in binding unrelated effector proteins.

Rab6-Rab6IP1-Rab11 Complex and the PLAT Domain

Beyond effector recruitment, an understanding of the biological function of Rab-effector complexes requires the crystallization

of more complete fragments of effector proteins. The Rab6-R1P complex, the largest Rab-effector structure determined to date, provides an opportunity to glean the possible contribution of the PLAT domain to Rab6IP1 function. The various roles ascribed to PLAT domains include binding to the β subunit of ATP synthase in sensory cilia of *C. elegans* (Hu and Barr, 2005) and membrane localization of lipoxygenases (Walther et al., 2002). The PLAT domain of the Rab6-R1P complex reveals a possible lipid-binding region (loops connecting β1-β2, β3-β4, and β5-β6; Figure S2) on the distal end of the molecule opposite the RUN1 domain. Superposition of the PLAT domains of several unrelated proteins suggests a topology for the β sandwich that would be consistent with a lipid-facing orientation. However, the role of the PLAT domain requires further clarification with lipid-binding studies, mutagenesis experiments, and vesicle trafficking assays. The tandem RUN1-PLAT domains are a rigid unit, as evidenced by extensive interactions between the proximal loops of the β sandwich and α9 of RUN1. In contrast, the low-resolution model of 12-lipoxygenase shows considerable flexibility in the linker between the PLAT domain and the catalytic domains (Aleem et al., 2008).

A GTP-dependent interaction between Rab11 and Rab6IP1 has been demonstrated using several approaches (Miserey-Lenkei et al., 2007). The overexpression of Rab6IP1 leads to a redistribution of peripheral Rab11 positive recycling endosomes toward the Golgi complex. This suggests the existence of ternary complexes between Rab6, Rab11, and Rab6IP1 (Miserey-Lenkei et al., 2007). A tentative hypothesis is that the PLAT domain of R1P might be interacting with membranes of recycling endosomes and participating together with Rab11 in the tethering of these membranes with Golgi membranes. Crystallization of the complete Rab6IP1 molecule along with Rab6/Rab11 in a ternary complex would provide further insight into the functional transport links between Golgi and endosomes.

EXPERIMENTAL PROCEDURES

Expression and Purification of Rab6-R1P

The RUN1-PLAT region (683–1061, henceforth referred to as R1P) of mouse Rab6IP1 was cloned into the Nde1/BamH1 site of the pET15 vector (ampicillin resistance). The recombinant protein lacked an affinity tag when expressed in *E. coli*. Human Rab6a (residues 8–195, Q72L) was cloned into the Nde1/Xho1 restriction sites of pET28 (kanamycin resistance), thus recombinant Rab6 contained an N-terminal His-tag (thrombin cleavage site). The two constructs were cotransformed into *E. coli* BL21(DE3) cells, and all subsequent small and large-scale cultures (including minimal media) were supplemented with 100 μg/ml ampicillin and 30 μg/ml kanamycin. Large-scale cultures were initially grown at 310 K in 2xYT media until the OD$_{600}$ was 0.6. The culture temperature was switched to 298 K and protein expression was induced by the addition of IPTG (0.2 mM) for approximately 6 hr. The cells were harvested by centrifugation at 4,000 rpm for 10 min and resuspended in 10 mM Tris-Cl (pH 8.0), 300 mM NaCl, 5 mM MgCl$_2$, 10 mM imidazole, and 10 mM β-mercaptoethanol (extraction buffer). The cells were sonicated and the lysates centrifuged at 20,000 × g for 30 min to eliminate insoluble protein and cellular debris. The Rab6-R1P complex was loaded onto Ni^{2+}-agarose (Chromatrin) via the N-terminal His-tag of Rab6. Following extensive washing with extraction buffer, the complex was eluted with a step gradient of 200 mM imidazole. Cleavage of the His-tag was performed in the presence of 10 units/mL of thrombin (GE Healthcare) overnight in dialysis sacs (10 mM Tris-Cl, 150 mM NaCl, 5 mM MgCl$_2$, 10 mM imidazole, and 10 mM β-mercaptoethanol [pH 8]). A second Ni^{2+}-agarose chromatography step was performed to eliminate uncleaved Rab6. Fractions containing the thrombin-cleaved complex were pooled, concentrated, and loaded onto a Superdex-200 size exclusion column (mounted on AKTAbasic FPLC, GE
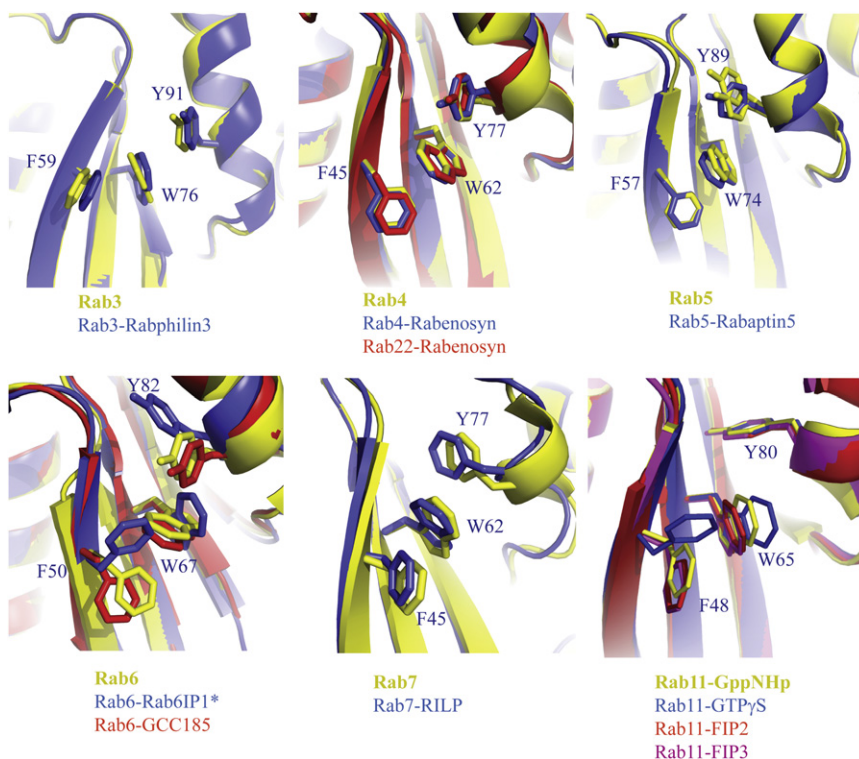
Figure 9. Hydrophobic Triads of Rabs Mediate Binding to Cognate Effectors

Yellow coloring corresponds to active Rab (GTP or analog) in the free state, whereas blue or red coloring indicates the conformation of the triad in the effector-bound state. The Rab6-R1P complex (*) is the exception to the general observation that the hydrophobic triads in the active (GTP) forms of Rabs do not undergo significant conformational changes upon binding to their cognate effectors. One other exception is Rab11, which exists in two alternate conformations at Phe48, depending on the presence of GppNHp or GTPγS (Protein Data Bank [PDB] codes 1yzk and 1oiw, respectively). Details of the side-chain conformational angles and the PDB codes of aligned structures are listed in Table S1.

free R value using a 10% randomly selected test set. Initial refinement consisted of torsion angle dynamics simulated annealing (Rice and Brünger, 1994) using the MLHL target function with the experimental phases as a prior phase distribution (Pannu et al., 1998), followed by model rebuilding using the graphic program COOT (Emsley and Cowtan, 2004). Later refinement consisted of iterative rounds of model building and selection of chemically reasonable water molecules in phased-combined σA-weighted $2F_o$-F_c maps, conjugate gradient minimization, and individual (isotropic) restrained atomic B-factor refinement with B-factor sharpening implemented in CNS version 1.2 (Brunger, 2007) using data between 50-3.2 Å resolution. Data and refinement statistics are shown in Table 1.

In the final Rab6-R1P model, Rab6a is ordered between Asp12-Met177. The R1P fragment (683–1066) is well defined for residues Asn713-Ala754, Asn759-Leu808, and Ala831-Glu1047. A large disordered loop connecting α2-α3 of RUN1 (residues Thr809-Ser830) is situated on the opposite side of RUN1 relative to the Rab6-binding face. Therefore, flexibility in this region does not complicate subsequent discussions of Ra6-R1P recognition.

Healthcare), equilibrated with 10 mM Tris-Cl, 100 mM NaCl, 5 mM MgCl₂, and 1 mM DTT (pH 7.5). The eluted complex was concentrated to 7–10 mg/ml before crystallization.

For the production of selenomethionine derivatized protein, recombinant expression was performed in the methionine auxotrophic *E. coli* strain B834(DE3). A 5 ml overnight culture in LB medium was used to inoculate a 0.5 l culture of M9 media, supplemented with vitamins, trace elements, and 40 mg/l of all amino acids except Met, according to the method of Van Duyne (Van Duyne et al., 1993). The culture was grown at 310 K to an OD₆₀₀ of 0.4. At this point, 100 mg/l SeMet was added and culture was switched to 298 K for an additional 30 min. Protein expression was induced with 0.2 mM IPTG and growth continued at 298 K for 8 hr. SeMet substituted protein was purified as before except for an increase in the concentration of β-mercaptoethanol (20 mM) and DTT (2 mM) to protect the SeMet residues from oxidation.

Crystallization, Data Collection, and Structure Determination

Crystals were grown by hanging drop vapor diffusion at 18°C. One microliter 7–10 mg/ml protein was mixed with one microliter mother liquor, consisting of 100 mM HEPES (pH 7.0), 2%–4% PEG 4000, and 3% 2,4-methypentanediol (MPD) on a siliconized coverslip. Hexagonal-shaped crystals grew to full size (0.4 × 0.15 × 0.15 mm) after 2 weeks. Crystals were cryoprotected in 100 mM HEPES (pH 7.0), 2%–4% PEG 4000, 3% MPD, and 25% glycerol, and then flash-frozen in liquid nitrogen.

The Rab6-R1P complex crystallized in space group P6₁22 with one complex in the asymmetric unit. SAD data were collected at the sulfur peak wavelength (0.978 Å, 100 K) on beamline BM14 (ESRF), whereas high-resolution native data for refinement were collected with a single native crystal on ID14-1 (ESRF). Data were processed using HKL2000, and intensities were reduced and scaled using SCALEPACK (Otwinowski and Minor, 1997). The initial phases and electron density map was obtained by SAD phasing using SOLVE (Terwilliger and Berendzen, 1999). Subsequent density modification involved solvent flattening (Wang, 1985) and histogram matching (Nieh and Zhang, 1999) as implemented in the Crystallography and NMR System (Brunger et al., 1998). Exploiting the positions of selenomethionine as anchors, the initial electron density maps allowed unambiguous chain tracing for most of the protein backbone, side chain, and GTP. Progress was monitored with the

Yeast Two-Hybrid Assays

Yeast two-hybrid tests were performed as previously described (Janoueix-Lerosey et al., 1995) using pLexA-Rab6a wt, pLexA-Rab6a T27N, pLexA-Rab6a I46E, and pLexA-Rab6a Q72L as baits. Rab6IP1 constructs (R1P, RUN1, RUN2; preys) were cloned into a pGAD vector.

In Vivo Analysis

Mutations K739E and Y908S+L911A were introduced into the pEGFPRab6IP1A plasmid using site-directed mutagenesis (QuickChange, Stratagene). The following oligonucleotides were used: Y908S+L911A mutant, sense oligonucleotide 5′-GAGCA-GTTCCTCTCTCACCTGGCCTCCTTCAACGCAGTG-3′; antisense oligonucleotide 5′-CACTGCGTTGAAGGAGGCCAGGTGAGAGAGG AACTGCTC-3′; K739E mutant, sense oligonucleotide 5′-GAATGTCGAAACAA GACCGAGAGGATGCTGGTAGAG-3′, antisense oligonucleotide CTCTACCA GCATCCTCTCGGTCTTGTTTC-GACATTC-3′. Cells were transfected for 48 hr and processed for immunofluorescence analysis as previously described (Miserey-Lenkei et al., 2007).

ACCESSION NUMBERS

The coordinates and structure factors have been deposited in the Protein Data Bank under the accession code 3CWZ.

Table 1. Data Collection and Refinement Statistics

	Selenomethionine	Native
Data Collection		
Space group	P6₁22	P6₁22
Cell dimensions	100.2, 299.3	99.9, 299.0
Wavelength (Å, Se peak)	0.978	0.934
Resolution (Å)	50-3.4	50-3.0
Completeness (%)	99.6 (100)	99.1 (98.6)
R_{merge} (%)	12.4 (72.0)	6.0 (80.0)
$I/\sigma(I)$ all data	—	13.3
$I/\sigma(I)$ > 3 (% of data)	88	85.8
Redundancy	22.9 (24.0)	9.2 (9.4)
Refinement		
Resolution	50-3.2	
Number of reflections	15,437	
Models	Rab6A (residues 12–177) R1P (713–754; 759–808; 831–1047)	
R_{work}/R_{free} (%)	24.8/30.1	
High-resolution shell	(31.6/35.6)	
Number of nonhydrogen atoms	3,902	
Protein	3,809	
GTP, ions	34	
Water	38	
Average B-factor	101.6 Å²	
Wilson plot	101.2 Å²	
Rms deviations		
Bond lengths (Å)	0.008	
Bond angles (°)	1.20	
Coordinate error (ESU, Å)	0.40	
Residues in Ramachandran		
Most favored region	87.4%	
Additionally allowed	12.1%	
Generously allowed	0.5%	
Disallowed	0%	

Values in parentheses correspond to the statistics for the highest resolution.

SUPPLEMENTAL DATA

Supplemental Data include two figures and two tables and can be found with this article online at http://www.cell.com/structure/supplemental/S0969-2126(08)00419-X.

REFERENCES

Aleem, A.M., Jankun, J., Dignam, J.D., Walther, M., Kuhn, H., Svergun, D.I., and Skrzypczak-Jankun, E. (2008). Human platelet 12-lipoxygenase, new findings about its activity, membrane binding and low-resolution structure. J. Mol. Biol. 376, 193–209.

Andres, D.A., Seabra, M.C., Brown, M.S., Armstrong, S.A., Smeland, T.E., Cremers, F.P., and Goldstein, J.L. (1993). cDNA cloning of component A of Rab geranylgeranyl transferase and demonstration of its role as a Rab escort protein. Cell 73, 1091–1099.

Bateman, A., and Sandford, R. (1999). The PLAT domain: a new piece in the PKD1 puzzle. Curr. Biol. 9, R588–R590.

Bergbrede, T., Pylypenko, O., Rak, A., and Alexandrov, K. (2005). Structure of the extremely slow GTPase Rab6A in the GTP bound form at 1.8A resolution. J. Struct. Biol. 152, 235–238.

Bourne, H.R., Sanders, D.A., and McCormick, F. (1991). The GTPase superfamily: conserved structure and molecular mechanism. Nature 349, 117–127.

Brass, A.L., Dykxhoorn, D.M., Benita, Y., Yan, N., Engelman, A., Xavier, R.J., Lieberman, J., and Elledge, S.J. (2008). Identification of host proteins required for HIV infection through a functional genomic screen. Science 319, 921–926.

Brunger, A.T. (2007). Version 1.2 of the crystallography and NMR system. Nat. Protoc. 2, 2728–2733.

Brunger, A.T., Adams, P.D., Clore, G.M., DeLano, W.L., Gros, P., Grosse-Kunstleve, R.W., Jiang, J.S., Kuszewski, J., Nilges, M., Pannu, N.S., et al. (1998). Crystallography and NMR system: a new software suite for macromolecular structure determination. Acta Crystallogr. D Biol. Crystallogr. 54, 905–921.

Burguete, A.S., Fenn, T.D., Brunger, A.T., and Pfeffer, S.R. (2008). Rab and Arl GTPase family members cooperate in the localization of the golgin GCC185. Cell 132, 286–298.

Callebaut, I., de Gunzburg, J., Goud, B., and Mornon, J.P. (2001). RUN domains: a new family of domains involved in Ras-like GTPase signaling. Trends Biochem. Sci. 26, 79–83.

Chavas, L.M., Torii, S., Kamikubo, H., Kawasaki, M., Ihara, K., Kato, R., Kataoka, M., Izumi, T., and Wakatsuki, S. (2007). Structure of the small GTPase Rab27b shows an unexpected swapped dimer. Acta Crystallogr. D Biol. Crystallogr. 63, 769–779.

Chavas, L.M., Ihara, K., Kawasaki, M., Kato, R., Izumi, T., and Wakatsuki, S. (2008). Purification, crystallization and preliminary X-ray crystallographic analysis of Rab27a GTPase in complex with exophilin4/Slp2-a effector. Acta Crystallogr. Sect. F Struct. Biol. Cryst. Commun. 64, 599–601.

Collins, R.N. (2005). Application of phylogenetic algorithms to assess Rab functional relationships. Methods Enzymol. 403, 19–28.

Cuif, M.H., Possmayer, F., Zander, H., Bordes, N., Jollivet, F., Couedel-Courteille, A., Janoueix-Lerosey, I., Langsley, G., Bornens, M., and Goud, B. (1999). Characterization of GAPCenA, a GTPase activating protein for Rab6, part of which associates with the centrosome. EMBO J. 18, 1772–1782.

Darchen, F., and Goud, B. (2000). Multiple aspects of Rab protein action in the secretory pathway: focus on Rab3 and Rab6. Biochimie 82, 375–384.

Del Nery, E., Miserey-Lenkei, S., Falguieres, T., Nizak, C., Johannes, L., Perez, F., and Goud, B. (2006). Rab6A and Rab6A' GTPases play non-overlapping roles in membrane trafficking. Traffic 7, 394–407.

Derby, M.C., Lieu, Z.Z., Brown, D., Stow, J.L., Goud, B., and Gleeson, P.A. (2007). The trans-Golgi network golgin, GCC185, is required for endosome-to-Golgi transport and maintenance of Golgi structure. Traffic 8, 758–773.

Eathiraj, S., Pan, X., Ritacco, C., and Lambright, D.G. (2005). Structural basis of family-wide Rab GTPase recognition by rabenosyn-5. Nature 436, 415–419.

Eathiraj, S., Mishra, A., Prekeris, R., and Lambright, D.G. (2006). Structural basis for Rab11-mediated recruitment of FIP3 to recycling endosomes. J. Mol. Biol. 364, 121–135.

Echard, A., Jollivet, F., Martinez, O., Lacapere, J.J., Rousselet, A., Janoueix-Lerosey, I., and Goud, B. (1998). Interaction of a Golgi-associated kinesin-like protein with Rab6. Science 279, 580–585.

Emsley, P., and Cowtan, K. (2004). Coot: model-building tools for molecular graphics. Acta Crystallogr. D Biol. Crystallogr. *60*, 2126–2132.

Farnsworth, C.C., Kawata, M., Yoshida, Y., Takai, Y., Gelb, M.H., and Glomset, J.A. (1991). C terminus of the small GTP-binding protein smg p25A contains two geranylgeranylated cysteine residues and a methyl ester. Proc. Natl. Acad. Sci. USA *88*, 6196–6200.

Fridmann-Sirkis, Y., Siniossoglou, S., and Pelham, H.R. (2004). TMF is a golgin that binds Rab6 and influences Golgi morphology. BMC Cell Biol. *5*, 18.

Fukuda, M. (2006). Rab27 and its effectors in secretory granule exocytosis: a novel docking machinery composed of a Rab27.effector complex. Biochem. Soc. Trans. *34*, 691–695.

Geyer, M., and Wittinghofer, A. (1997). GEFs, GAPs, GDIs and effectors: taking a closer (3D) look at the regulation of Ras-related GTP-binding proteins. Curr. Opin. Struct. Biol. *7*, 786–792.

Gillmor, S.A., Villasenor, A., Fletterick, R., Sigal, E., and Browner, M.F. (1997). The structure of mammalian 15-lipoxygenase reveals similarity to the lipases and the determinants of substrate specificity. Nat. Struct. Biol. *4*, 1003–1009.

Goldfinger, L.E. (2008). Choose your own path: specificity in Ras GTPase signaling. Mol. Biosyst. *4*, 293–299.

Goody, R.S., Rak, A., and Alexandrov, K. (2005). The structural and mechanistic basis for recycling of Rab proteins between membrane compartments. Cell. Mol. Life Sci. *62*, 1657–1670.

Grigoriev, I., Splinter, D., Keijzer, N., Wulf, P.S., Demmers, J., Ohtsuka, T., Modesti, M., Maly, I.V., Grosveld, F., Hoogenraad, C.C., et al. (2007). Rab6 regulates transport and targeting of exocytotic carriers. Dev. Cell *13*, 305–314.

Hu, J., and Barr, M.M. (2005). ATP-2 interacts with the PLAT domain of LOV-1 and is involved in Caenorhabditis elegans polycystin signaling. Mol. Biol. Cell *16*, 458–469.

Jagoe, W.N., Lindsay, A.J., Read, R.J., McCoy, A.J., McCaffrey, M.W., and Khan, A.R. (2006). Crystal structure of rab11 in complex with rab11 family interacting protein 2. Structure *14*, 1273–1283.

Janoueix-Lerosey, I., Jollivet, F., Camonis, J., Marche, P.N., and Goud, B. (1995). Two-hybrid system screen with the small GTP-binding protein Rab6. Identification of a novel mouse GDP dissociation inhibitor isoform and two other potential partners of Rab6. J. Biol. Chem. *270*, 14801–14808.

Kukimoto-Niino, M., Takagi, T., Akasaka, R., Murayama, K., Uchikubo-Kamo, T., Terada, T., Inoue, M., Watanabe, S., Tanaka, A., Hayashizaki, Y., et al. (2006). Crystal structure of the RUN domain of the RAP2-interacting protein x. J. Biol. Chem. *281*, 31843–31853.

Mallard, F., Tang, B.L., Galli, T., Tenza, D., Saint-Pol, A., Yue, X., Antony, C., Hong, W., Goud, B., and Johannes, L. (2002). Early/recycling endosomes-to-TGN transport involves two SNARE complexes and a Rab6 isoform. J. Cell Biol. *156*, 653–664.

Merithew, E., Hatherly, S., Dumas, J.J., Lawe, D.C., Heller-Harrison, R., and Lambright, D.G. (2001). Structural plasticity of an invariant hydrophobic triad in the switch regions of Rab GTPases is a determinant of effector recognition. J. Biol. Chem. *276*, 13982–13988.

Miserey-Lenkei, S., Couedel-Courteille, A., Del Nery, E., Bardin, S., Piel, M., Racine, V., Sibarita, J.B., Perez, F., Bornens, M., and Goud, B. (2006). A role for the Rab6A' GTPase in the inactivation of the Mad2-spindle checkpoint. EMBO J. *25*, 278–289.

Miserey-Lenkei, S., Waharte, F., Boulet, A., Cuif, M.H., Tenza, D., El Marjou, A., Raposo, G., Salamero, J., Heliot, L., Goud, B., et al. (2007). Rab6-interacting protein 1 links Rab6 and Rab11 function. Traffic *8*, 1385–1403.

Mori, T., Wada, T., Suzuki, T., Kubota, Y., and Inagaki, N. (2007). Singar1, a novel RUN domain-containing protein, suppresses formation of surplus axons for neuronal polarity. J. Biol. Chem. *282*, 19884–19893.

Nieh, Y.P., and Zhang, K.Y. (1999). A two-dimensional histogram-matching method for protein phase refinement and extension. Acta Crystallogr. D Biol. Crystallogr. *55*, 1893–1900.

Ogura, K., Shirakawa, M., Barnes, T.M., Hekimi, S., and Ohshima, Y. (1997). The UNC-14 protein required for axonal elongation and guidance in Caeno-rhabditis elegans interacts with the serine/threonine kinase UNC-51. Genes Dev. *11*, 1801–1811.

Opdam, F.J., Echard, A., Croes, H.J., van den Hurk, J.A., van de Vorstenbosch, R.A., Ginsel, L.A., Goud, B., and Fransen, J.A. (2000). The small GTPase Rab6B, a novel Rab6 subfamily member, is cell-type specifically expressed and localised to the Golgi apparatus. J. Cell Sci. *113*, 2725–2735.

Ostermeier, C., and Brunger, A.T. (1999). Structural basis of Rab effector specificity: crystal structure of the small G protein Rab3A complexed with the effector domain of rabphilin-3A. Cell *96*, 363–374.

Otwinowski, Z., and Minor, W. (1997). Processing of X-ray diffraction data collected in oscillation mode. In Methods in Enzymology, Volume 276: Macromolecular Crystallography, part A, C.W. Carter, Jr. and R.M. Sweet, eds. (New York: Academic Press), pp. 307–326.

Pannu, N.S., Murshudov, G.N., Dodson, E.J., and Read, R.J. (1998). Incorporation of prior phase information strengthens maximum-likelihood structure refinement. Acta Crystallogr. D Biol. Crystallogr. *54*, 1285–1294.

Ponting, C.P., Hofmann, K., and Bork, P. (1999). A latrophilin/CL-1-like GPS domain in polycystin-1. Curr. Biol. *9*, R585–R588.

Rice, L.M., and Brünger, A.T. (1994). Torsion angle dyamics: reduced variable conformational sampling ehaces crystallographic structure refiement. Proteins *19*, 277–290.

Sandford, R., Sgotto, B., Aparicio, S., Brenner, S., Vaudin, M., Wilson, R.K., Chissoe, S., Pepin, K., Bateman, A., Chothia, C., et al. (1997). Comparative analysis of the polycystic kidney disease 1 (PKD1) gene reveals an integral membrane glycoprotein with multiple evolutionary conserved domains. Hum. Mol. Genet. *6*, 1483–1489.

Shiba, T., Koga, H., Shin, H.W., Kawasaki, M., Kato, R., Nakayama, K., and Wakatsuki, S. (2006). Structural basis for Rab11-dependent membrane recruitment of a family of Rab11-interacting protein 3 (FIP3)/Arfophilin-1. Proc. Natl. Acad. Sci. USA *103*, 15416–15421.

Short, B., Preisinger, C., Schaletzky, J., Kopajtich, R., and Barr, F.A. (2002). The Rab6 GTPase regulates recruitment of the dynactin complex to Golgi membranes. Curr. Biol. *12*, 1792–1795.

Stenmark, H., and Olkkonen, V.M. (2001). The Rab GTPase family. Genome Biol. *2*, REVIEWS3007.

Teber, I., Nagano, F., Kremerskothen, J., Bilbilis, K., Goud, B., and Barnekow, A. (2005). Rab6 interacts with the mint3 adaptor protein. Biol. Chem. *386*, 671–677.

Terwilliger, T.C., and Berendzen, J. (1999). Automated MAD and MIR structure solution. Acta Crystallogr. D Biol. Crystallogr. *55*, 849–861.

Van Duyne, G.D., Standaert, R.F., Karplus, P.A., Schreiber, S.L., and Clardy, J. (1993). Atomic structures of the human immunophilin FKBP-12 with FK506 and rapamycin. J. Mol. Biol. *229*, 105–124.

Walther, M., Anton, M., Wiedmann, M., Fletterick, R., and Kuhn, H. (2002). The N-terminal domain of the reticulocyte-type 15-lipoxygenase is not essential for enzymatic activity but contains determinants for membrane binding. J. Biol. Chem. *277*, 27360–27366.

Wang, B.C. (1985). Resolution of phase ambiguity in macromolecular crystallography. Methods Enzymol. *115*, 90–112.

White, J., Johannes, L., Mallard, F., Girod, A., Grill, S., Reinsch, S., Keller, P., Tzschaschel, B., Echard, A., Goud, B., et al. (1999). Rab6 coordinates a novel Golgi to ER retrograde transport pathway in live cells. J. Cell Biol. *147*, 743–760.

Wu, M., Wang, T., Loh, E., Hong, W., and Song, H. (2005). Structural basis for recruitment of RILP by small GTPase Rab7. EMBO J. *24*, 1491–1501.

Wu, S.K., Zeng, K., Wilson, I.A., and Balch, W.E. (1996). Structural insights into the function of the Rab GDI superfamily. Trends Biochem. Sci. *21*, 472–476.

Zerial, M., and McBride, H. (2001). Rab proteins as membrane organizers. Nat. Rev. Mol. Cell Biol. *2*, 107–117.

Zhu, G., Zhai, P., Liu, J., Terzyan, S., Li, G., and Zhang, X.C. (2004). Structural basis of Rab5-Rabaptin5 interaction in endocytosis. Nat. Struct. Mol. Biol. *11*, 975–983.